INTER-AMERICAN TROPICAL TUNA COMMISSION

***AD-HOC* PERMANENT WORKING GROUP ON FADS**

8TH MEETING

La Jolla, California (USA)
07-08 June 2024

DOCUMENT FAD-08-02

ECHOSOUNDER BUOY DERIVED TROPICAL TUNA BIOMASS INDICES IN THE EASTERN PACIFIC OCEAN

Jon Uranga[1], Jon Lopez[2], Maitane Grande[1], Cleridy E. Lennert-Cody[2], Iñaki Quincoces[1], Mark N. Maunder[2], Alexandre Aires-da-Silva[2], Gorka Merino[1], Hilario Murua[3], Josu Santiago[1]

CONTENTS

EXECUTIVE SUMMARY

The collaboration with certain tropical tuna vessel-owners associations and buoy manufacturers operating in the eastern Pacific Ocean provided access to information collected by their satellite-linked echosounder buoys since 2012. These instrumented buoys provide fishers with remote real-time geolocation and fish abundance information underneath fish aggregating devices (FADs). Echosounder buoys serve, therefore, as effective observation platforms of the pelagic environment and offer the possibility of assessing tuna abundance at FADs in a cost-effective catch-independent manner. However, current echosounder buoys provide a single biomass value and do not discriminate between species or consider size composition of the fish. Therefore, to obtain specific species indices, the echosounder buoy data must be currently combined with fishery data, in particular, species and size composition information. In this paper, we present an updated estimation of abundance indices for skipjack, yellowfin and bigeye tuna in the eastern Pacific Ocean using echosounder buoys data for the 2012-2023. These indices were used in the IATTC benchmark stock assessments of skipjack tuna and explored for bigeye and yellowfin tuna assessments in 2024.

[1] AZTI, Marine Research, Basque Research and Technology Alliance (BRTA). Txatxarramendi ugartea z/g, 48395. Sukarrieta - Bizkaia, Spain
[2] Inter-American Tropical Tuna Commission, 8901 La Jolla Shores Drive, La Jolla CA 92037, USA
[3] International Seafood Sustainability Foundation (ISSF), 3706 Butler Street Suite #316, 15201-1820 Pittsburgh, PA (USA) hmurua@iss-foundation.org

1. INTRODUCTION

Historically, tropical tuna stock assessments have almost exclusively relied on abundance indices that depend on commercial catches and fishing effort obtained from captain's logbooks or observer data (Maunder and Punt 2004). These data are integrated into fish stock assessment models to evaluate the state and evolution of fish stocks, providing information on relative trends in fish abundance (Quinn and Deriso 1999). These trends are often monitored with Catch-Per-Unit-Effort (CPUE) based relative abundance indices, which are related to abundance through the catchability coefficient (q). However, various factors such as changes in fishing efficiency, species or fleet spatial dynamics, and environmental conditions can affect this proportionality (Maunder and Punt 2004; Maunder et al. 2006). Therefore, CPUE standardization is used to eliminate these effects and identify changes related to population abundance.

The incorporation of new technologies and the massive use of Fish Aggregating Devices (FADs) have led to a significant increase in fishing efficiency of the tropical tuna purse-seine fishery (Lopez et al. 2014; Torres-Irineo et al. 2014; Gaertner et al. 2016). However, scientists face challenges in standardizing FAD fishing CPUE due to the difficulties associated to the lack of a good proxy for purse seine effort and the inclusion of fine scale covariates that reflect technological changes and effort creep of the fishery (Gaertner et al. 2016; Katara 2018; Wain 2021). Consequently, the purse-seine FAD CPUE has not generally been included in tropical tuna stock assessment models in the eastern Pacific Ocean (EPO). However, successful science-industry collaborative projects have begun to provide valuable information on the adoption of technological advances for the tropical tuna purse seine fleet to improve the CPUE standardization process (Wain 2021), and ultimately, tropical tuna assessments.

The introduction of satellite-linked echosounder buoys attached to FADs in regular fishing operations (Scott 2014) offers an alternative method to observe the dynamics of aggregations at FADs and estimate catch-independent indices. These instrumented buoys provide fishers with real time information on the FAD position and a rough estimate of the fish biomass underneath them, making them cost effective observation platforms for remotely monitoring tuna and other species aggregations in a systematic non-invasive way. In recent years, industry-research collaborations have allowed for the collection of buoy-derived data, and scientific methodological frameworks have been developed to extract reliable information from these data (e.g., Orúe et al., 2019). This information has proven to be useful for scientific research, enabling a variety of investigations on tuna behaviour and ecology around FADs and the development of buoy-derived abundance indices, among others (e.g., Lopez et al. 2014; Capello et al. 2016; Moreno 2016; Orúe et al., 2019; Santiago et al. 2019; Baidai 2020). Results of this collaborative effort were first presented at the 5th FAD working group (FADWG) of the IATTC.

Building on this achievement, a collaborative framework was established between the Inter-American Tropical Tuna Commission (IATTC) and AZTI, in partnership with echosounder buoy providers and some of the of tropical tuna purse seiner fishing companies operating in the EPO (i.e., companies integrated in the vessel owner associations OPAGAC-AGAC and Cape Fisheries), with the special support of the International Seafood Sustainability Foundation (ISSF). In recent years (Santiago et al. 2019, Santiago et al. 2020, Santiago et al. 2020b, Santiago et al. 2021, Uranga et al. 2024), echosounder buoy-based abundance indices (BAI) were developed for the three main tropical tuna (yellowfin, bigeye, and skipjack) assessments in the Atlantic Ocean. Similarly, the BAI index was integrated into the IATTC's interim skipjack assessments in 2022 (SAC-13-07). The buoy index developed for skipjack was used in the 2024 benchmark assessments of the IATTC, and explored, for inclusion, in the bigeye and yellowfin tuna assessments (see SAC-15-02, SAC-15-03 and SAC-15-04 for details).

This paper presents updated abundance indices for tropical tuna species in the EPO using echosounder buoy data from 2012 to 2023 and describes the progress made since the last update of the indices, as well as discusses future improvements of the methodology.

2. MATERIAL AND METHODS

2.1 Acoustic data pre-filtering

The primary data used in this analysis was collected by satellite-linked echo-sounder buoys attached to FADs in the EPO tropical tuna purse-seine fishery. Because authors have developed methods to estimate biomass estimates per species for Satlink buoys (e.g., Orue et al. 2019), only data collected by this buoy manufacturer was used in this analysis. Technical specifications for each buoy model are presented in Table 1. The buoys record information from a depth of 3 to 115 meters, divided into ten uniform vertical layers, each with a resolution of 11.2 meters. Note that the first 3 meters are considered the blind zone and do not provide usable data. Five different buoy models (DS+, DSL, ISD, ISL, and SLX) were used during the analyzed period (2012 to 2023) (Table 1).

The time-series from 2012 to 2023 contains two main types of information: i) historic data (2012-2021) voluntarily reported by fishing companies such as Albacora, Calvo, Garavilla, Ugavi, and Cape Fisheries, as well as ii) recent data (2022-2023) reported by the whole fleet under Resolution C-21-04. The historic data contains information from a total of 23 purse-seine vessels and 5 CPCs (Panama, Spain, Ecuador, El Salvador, USA). The data for the most recent years (i.e., 2022-2023) includes information for the whole EPO operational fleet, significantly increasing the number of vessels and CPCs (a total of 162 vessels, 8 CPCs) and expanding the study area Figure 1.

The database used for this analysis included a total of 38.9 million acoustic records from 62382 individual buoys. We excluded data from the first semester of 2012 due to the low number of records available (see Figure 1). Additionally, acoustic records from areas with a low number of observations (less than 30 records in 5ºx5º statistical rectangles) and those west of 150ºW were excluded from this analysis.

From each single data record, transmitted by the buoy via satellite, the following information was extracted: "*Name*", unique alphanumeric identification of the buoy, given by the model code (DS+, DSL, ISL, ISD, SLX) followed by 5-6 digits; "*OwnerName*", name of the buoy owner assigned to a unique purse seine vessel; "*MD*", message descriptor (160, 161 and 162 for position data, without echosounder data, and 163, 168, 169 and 174 for echosounder data); "*StoredTime*", date (dd/mm/yyyy) and hour (HH:MM) of the position and the echosounder records; "*Latitude, Longitude*", record-associated GPS location information (in decimal degrees); "*Bat*", battery charge level of the buoy, as a percentage (not provided, except for the D+ and DS+ models, in voltage); "*Speed*", estimated speed of the buoy in knots; "*Layer1-Layer10*", estimated tons of tuna by layer (values are estimated based on the manufacturer´s method that converts raw acoustic backscatter into biomass in tons, using a depth layer echo-integration procedure based exclusively on an algorithm using the target strength (TS) and weight of skipjack tuna); "*Sum*", sum of the biomass estimated for all layers; "*Max*", maximum biomass estimated at any layer; and "*Mag1, Mag3, Mag5 and Mag7*", magnitudes corresponding to the counts of detected targets according to the TS of the detection peak.

A set of five filters were applied to the original data to eliminate artifacts: 1) isolated, duplicated, and ubiquitous rows, which are often caused by satellite communication issues; 2) buoys located within 1 km of land or in continental shelf areas (i.e., those in fishing ports or with bottom depths shallower than 200 m), which were identified and removed using shoreline data from the GSHHG database (Wessel 1996) and a worldwide global bathymetry information (Amante and Eakins 2009); and 3) "on-board" or "at sea" positions, which were identified using a Random Forest algorithm (Orue et al. 2019; Santiago et al. 2020). These cases typically occur when a buoy is activated onboard a vessel prior to deployment or post-retrieval.

In addition to the data cleaning filters mentioned earlier, the following selection criteria (Santiago et al. 2020) were used to create the final dataset for the standardization analysis. Firstly, shallower layers (<25m) were excluded because as they are considered to potentially reflect non-tuna species (e.g., Orue et al. 2019). Secondly, only data recorded around sunrise, between 4 a.m. and 8 a.m., in local time, were considered for the analysis as they are believed to better capture the biomass under the FADs (e.g., Moreno et al. 2007 and FAD-06-01 – the hours around sunrise are preferred setting times for fishers on FADs). Finally, acoustic data belonging to “virgin segments” were selected to use the segment of a buoy trajectory whose associated FAD likely represents a new deployment that has been potentially colonized by tuna and not fished yet. To calculate virgin segments, single buoy information was divided into smaller segments where the difference between two consecutive observations of the same buoy was larger than 30 days. Although this may represent buoys that have been re-deployed, it seems unlikely as redeployments usually happen in a short time window. Segments with less than 30 observations and those having a time difference between any of the consecutive observations longer than 4 days during the first 35 days were removed. Finally, from the remaining data, information corresponding to 20-35 days at sea was used as this is the time period for which FADs seem to be colonized (Orue et al. 2019). Figure 2 shows a diagram with an example of “virgin” segments used to calculate the BAI index.

2.2 From acoustic data to a species-specific abundance indicator

To calculate the biomass aggregated under a FAD from the acoustic signal, Satlink uses the Target Strength (TS) of one species, skipjack, to provide the biomass in tons, and thus, biomass data from Satlink has to be converted to decibels (acoustic information) reversing their formula for the biomass computation. Once the raw acoustic information is available, this can be recomputed into biomass per species using standard acoustic abundance estimation equations (Simmons and MacLennan 2005):

$$Biomass_i = \frac{s_V \cdot Vol \cdot p_i}{\sum_i \sigma_i \cdot p_i}$$

where s_V is the volume backscattering strength, *Vol* is the sampled volume of the beam and p_i and σ_i are the proportion and linearized target strength of each species *i* respectively.

Species proportions in weight at 1°x1° and month resolution were extracted from logbooks (for class 1-5 vessels, ≤ 363 mt) and observers data (for class 6 vessels, >363mt) for 14 flags. Mean fish lengths (L_i), for 5°x5° area - month resolution were obtained from IATTC port-sampling data for skipjack (SKJ), bigeye (BET) and yellowfin (YFT), which were raised to the catch in the sampled wells. Weights were estimated using IATTC weight-length conversion factors. Then, the following Target Strength-length relationships were used to obtain linearized TS per kilogram:

$$\sigma_i = \frac{10^{(TS)/10}}{w_i}$$

where w_i is the mean weight of each species and TS is the backscattering cross-section of each species individual fish. The linear value of TS is assumed to be proportional to the square of the fish length (Simmons and MacLennan 2005).

$$TS = 20log(Li) + b20$$

Given that each brand uses different operating frequencies, we used different b20 values for each species (b20 is the so-called reduced target strength). The b20 values were obtained from Boyra et al. (2018) for SKJ, from Sobradillo et al. (2024) for YFT, and from Boyra et al. (2018) for BET.

To obtain information on catch composition and fish size for the corresponding time-area strata of acoustic records, the previous three-step hierarchical process was updated into a higher-resolution five-step hierarchical approach. First, the species distribution data from the same 1°x1° grid, year, and month was used. If this data was unavailable, the species distribution data from the same 5°x5° grid, year, and month was used. In a third level, the spatial window was expanded, and the specific areas defined by IATTC staff for the assessments of skipjack (A), bigeye (B), and yellowfin tropical tuna (C), based on catches and the fishery structure of the floating object fishery. In a fourth level, data was aggregated by quarter and 5°x5° grid. Finally, if previous options were not available, mean values were used at a quarterly and regional resolution, as shown in Figure 3.

It is important to note that the first level does not apply to fish size as size frequency data is only available at 5°x5° resolution.

The results presented in this document specifically pertain to the fraction of the acoustic signal estimated to be informative for the biomass of the tree main tropical tuna species.

2.3 The BAI index: Buoy-derived Abundance Index

The buoy abundance index, BAI, was determined as the 0.9 quantile of the integrated acoustic energy observations in each of the "virgin" sequences. A high quantile was chosen because it is likely that large values are produced by tuna, as opposed to other species. This assumption is also used by all buoy manufacturers in the market, who use the maximum value as the biomass summary for each time interval. In this study, a high quantile was selected instead of the maximum to provide a more robust estimator by removing outlier values. The total number of "virgin" sequences analyzed, and hence the number of observations included in the model, was 7671, of which 7.595 (99%) had positive values.

2.4 The statistical model

The covariates used in the standardization process and fitted as categorical variables were year-quarter, 5x5º area, and buoy model. Additionally, a proxy of 1ºx1º and monthly FAD densities and the following environmental variables were included as continuous variables in the model: ocean mixed layer thickness, chlorophyll, sea surface temperature (SST), and SST and chlorophyll fronts. The model assumes that the signal from the echosounder buoy is proportional to the abundance of fish under the FAD, which is similar to the fundamental relationship between CPUE and abundance used in quantitative fisheries analysis.:

$$BAI_t = \varphi \, . B_t$$

where BAI_t is the Buoy-derived Abundance Index and B_t is the abundance in time t (Santiago et al., 2016).

Although it would appear to be obvious, there is not a lot of literature available on the relationship between acoustic indicators and fishing performance. In general, it is assumed that acoustic echo-integration is a linear process, i.e., proportional to the number of targets (Simmons and MacLennan 2005) and has been experimentally proven to be correct with some limitations (Foote, 1983; Røttingen, 1976). Therefore, acoustic data (via echo-integration) are commonly taken as a proxy for abundance and are used to obtain acoustic estimates of abundance for many pelagic species (Hampton 1996; ICES 2015; Masse et al. 2018).

As with catchability, the coefficient of proportionality (ϕ) is not constant for many reasons. In order to ensure that ϕ can be assumed to be constant (i.e., to control the effects other than those caused by changes in the abundance of the population) a standardization analysis should be performed by aiming to remove factors other than changes in abundance of the population. This can be performed standardizing nominal measurements of the echosounder buoy using a Generalized Linear Mixed Modelling (GLMM) approach.

In this analysis, log (BAI+k) with a normal distribution was used as the response variable. A small constant k was added to the response variable to allow for modelling observations with zero values. The constant k was set as the detection threshold of the echo-sounder buoy (k = 0.001). It is known that this type of approach may cause some bias in the estimation of the year-quarter effect (Hinton and Maunder, 2004). However, the number of zeros in the dataset is relatively low (around 1%) in this analysis and therefore the bias is expected to be non-significant. A GLMM with a log-normal error structured model was applied to standardize the acoustic observations. A stepwise procedure was used to fit the model with all the explanatory variables and interactions in order to determine those that significantly contributed to explaining the variability in the data. Deviance analysis and summary tables were created, and the final selection of explanatory variables was conducted using: a) the relative percent increase in deviance explained when the variable was included in the model (variables that explained more than 5% were selected), and b) The Chi-square ($\chi 2$) significance test.

Interactions between the temporal component (year-quarter) with the rest of the variables were also evaluated. If an interaction was statistically significant, it was then considered as a random interaction(s) within the final model (Maunder and Punt 2004).

The selection of the final model was based on the Akaike's Information Criterion (AIC), the Bayesian Information Criterion (BIC), and a Chi-square ($\chi 2$) test of the difference between the log- likelihood statistic of different model formulations. The year-quarter effect least square means (LSmeans) were bias corrected for the logarithm transformation algorithms using the approach described in Lo et al. 1992. All analyses were done using the lme4 package in R (Bates et al. 2014).

3. RESULTS

A total of 38.9million acoustic records were evaluated from 62382buoys spanning from 2012 to 2023, resulting in 7671observations for the GLMM analysis. Each observation was calculated as the 90th percentile of a "virgin" segment of buoy trajectories. As explained above, a virgin segment represents a deployment that has the potential to be colonized by tuna but has not yet been fished.

Skipjack-specific results are presented in this document To better illustrate the statistical analyses, the nature of the data and spatial distribution, as well as the derived BAI index. However, in Table 3 and Figure 9, the results for all three main tropical tuna species in the eastern Pacific Ocean are presented.

Figure 4 displays histograms of the BAI and log-transformed BAI nominal values for the skipjack model. The log transformation was applied to make the data follow a normal distribution, as shown in the left panel of Figure 4. Figure 5 displays the spatial distribution of the number of "virgin" segments of buoy trajectories that were used in the GLMM analysis on a 5ºx5º grid. The quarterly evolution of the number of observations on a 5^{o}x5^{o} grid is shown in Figure 6. Figure 7 illustrates the quarterly evolution of the nominal log BAI index for SKJ by squares of 5x5 degrees from the second semester of 2012 to 2023.

The results of the deviance analysis for the SKJ model are presented in Table 2. The model explained 41,2% of the total deviance, and the most significant explanatory variables were year-quarter, 5^{o}x5^{o} area, and the interaction between year-quarter and area, which was considered a random effect. No significant residual patterns were observed (Figure 8).

Quarterly series of standardized species-specific BAI indices are presented in Table 3 and Figure 9. For SKJ tuna, again as an illustrative example, three periods showed higher values: a) from the start of the series in 2012 until 2013; b) from the second half of 2019 to the end of the first half of 2020; and c) starting from the second quarter of 2022 up to the second half of 2023.The coefficients of variation remained relatively stable throughout the time series at levels of 22-29%.

4. DISCUSSION

This paper presents the results of the tropical tuna buoy-derived abundance indices in the eastern Pacific Ocean. The series has been updated with data up to 2023, including voluntary data reported by certain companies from 2012-2021, as well as mandatory data reporting requirements for the whole fleet under Resolution C-21-04 for 2022-2023. For this study, we adapted the methodology previously outlined for tropical tuna populations in the Pacific and other oceans (Santiago et al. 2019, Santiago et al. 2020a, Santiago et al. 2020b, Uranga et al. 2022, Uranga et al. 2023). As such, some of the identified areas for improvement from previous years were addressed, and new hierarchical methodological inputs were implemented to better consider data resolution needs and the specifications of each fishery area and structure of the floating object fishery in the eastern Pacific Ocean.

Data collection

To improve the consistency of the abundance indices generated so far, it would be beneficial to compile historic acoustic data from as many companies or associations as possible and integrate them into previously established indices for earlier years. Current results were obtained under the assumption that the data may represent a single population; however, this year's update includes a number of observations in coastal areas due to the inclusion of data from the entire fleet in 2022 and 2023. The potential similarities or discrepancies between inshore and offshore indicators and indices, when developed, must be further investigated to better understand the factors that may affect the acoustic signal and determine whether it should be treated as a single index or multiple separate indices. Similarly, this aligns with the need for the index to accurately represent catch-composition and abundances in different species-specific areas as defined by the fishery structure analyses conducted by the staff. In this study, the three specific areas were used (Figure 3) for the main tropical tuna species, and these were applied to the entire series. However, fisheries and species are dynamic and ideally, methods that estimate species and size composition from the acoustic signal should be developed to obtain indices that are more independent from fisheries data.

In addition to time series considerations, data collection also varies between the different buoy manufacturers. These differences need to be considered, solved, and incorporated into future analyses to develop a more comprehensive buoy-derived index of abundance. As such, the fundamental acoustic data variability in data collection needs to be explored, and intercalibration methods developed and implemented so that acoustic signals from different buoy models and manufacturers are comparable and methods are as flexible as possible to account for any differences that may arise from buoy-related data submissions.

Methodology Update

In previous analyses, we recognized the need to review the filters used to clean the database of artifacts and assess their suitability for trajectories generated by different approaches. This task should be prioritized in the near future.

As outlined in the materials and methods section, we updated the hierarchical protocol for matching specific catch composition and size data to acoustic data, so that the method is more inclusive and higher-resolution levels are considered. In the coming years, new models that enhance the robustness of estimating specific catch and size compositions across space and time should be developed. Establishing geospatial or machine learning models may improve the information available for specific catch and size composition under FADs, both temporally and spatially. Additionally, the relationship between catch composition and the colonization process should be better understood, as well as studies that consider the vertical behavior of different species should be conducted to potentially refine acoustic measurements and their interpretation, by area and season. In this regard, incorporating data from electronic tagging studies could help define the time typically spent by different species and sizes at each depth in space and time.

Regarding colonization models, the assumption of the 20-35 days after new deployments (based on Orue et al., 2019) should be tested. Ideally, adaptive approaches that suits different regions and seasons should be explored, where the colonization curves will be independently estimated and incorporated in the model for each individual FAD or observation. To achieve this, FAD logbook and observer data, along with buoy data, are being explored, as well as novel approaches that define single trajectories from raw data are being considered via the revision of, among others, the parameters used to filter, process and remove artifacts from the data.

Regarding the model used to standardize nominal biomass values, sensitivity tests should be conducted to assess the effect of using different metrics (i.e., mean, median, 90th percentile, etc.) in the final index of abundance. Similarly, various virgin segment classification thresholds should be tested, along with different catch compositions resolutions. Moreover, including variables other than those presented in this document should be explored in the model building phase (e.g., additional environmental variables) to try to improve model performance and diagnostics.

Progress in acoustics and future lines

Aside from improving the methodology for estimating biomass, it is important to continue exploring the idea of cross-referencing acoustic data with catch data of the corresponding buoy. This process is key for better understanding, in fine detail, the variability of the data and its interpretation, ultimately enhancing its reliability and developing methods to account for such variability. Also, transitioning from specific measurements extracted from the virgin segment, following the steps and assumptions outlined in this document, to the use of complete echograms of the virgin segment as inputs for the models can lead to substantial qualitative improvements. In this regard, ways to increase the number of samples comparing echograms with their associated catches should be established, as machine learning or computer vision models that rely on images require large datasets to reliably identify patterns. Additionally, experiments should be conducted to assess whether multifrequency buoys and data can be used to improve data collection and species and size discrimination. In fact, the ability to discriminate skipjack (a species without a swim bladder and the main target of the FAD fishery) from species with swim bladders (bigeye and yellowfin, often non-target species at FADs) would be a significant step towards both science and sustainable management of tropical tuna.

All specific points for improvement identified in this study highlight the need for further research in developing abundance indices based on buoy acoustics. The network of FADs equipped with buoy acoustics could be, indeed, a global monitoring tool of the pelagic environment that provides substantial information about the three main tropical tuna species in a catch-independent, systematic and cost-effective manner. The success of using echosounder buoy data heavily depends on effectively managing the noisy nature of it, which involves filtering out acoustic data not pertinent to significant tuna presence and developing approaches that maximize the potential of this valuable source of information. Looking ahead, it would be beneficial to engage in collaborative projects with the fishing fleet to collect acoustic data both via the reporting of historic buoy information or conducting experiments that rely on the vessels' acoustic devices (i.e., echosounders and sonars). These acoustic devices, installed on most of the tropical tuna purse seine vessels operating in the EPO, can provide high resolution acoustic data and offer complementary information about the morphology and dynamics of the schools associated with FADs, potentially transforming fishing vessels into research platforms.

ACKNOWLEDGEMENTS

We want to express our gratitude to the following fishing companies that have provided historic acoustic information from their echosounder buoys: Albacora, Calvo, Garavilla, Ugavi and Cape Fisheries. The authors also want to thank the Basque Government and ISSF for supporting this work.

REFERENCES

Amante, C. and B. Eakins (2009). "ETOPO1 1 arc-minute global relief model: procedures, data sources and analysis. NOAA Technical Memorandum NESDIS NGDC-24." National Geophysical Data Center, NOAA 10: V5C8276M.

Baidai, Y. D. A. (2020). Derivation of a direct abundance index for tropical tunas based on their associative behavior with floating objects, Université Montpellier.

Bates, D., M. Mächler, et al. (2014). "Fitting linear mixed-effects models using lme4." arXiv preprint arXiv:1406.5823.

Belkin, I. M. and J. E. O'Reilly (2009). "An algorithm for oceanic front detection in chlorophyll and SST satellite imagery." Journal of Marine Systems 78(3): 319-326.

Bertrand, A. and E. Josse (2000). "Tuna target-strength related to fish length and swimbladder volume." ICES Journal of Marine Science 57(4): 1143-1146.

Boyra, G., G. Moreno, et al. (2018). "Target strength of skipjack tuna (Katsuwanus pelamis) associated with fish aggregating devices (FADs)." ICES Journal of Marine Science 75(5): 1790-1802.
Capello, M., J. L. Deneubourg, et al. (2016). "Population assessment of tropical tuna based on their associative behavior around floating objects." Scientific Reports 6(1): 36415.
Gaertner, D., J. Ariz, et al. (2016). "Objectives and first results of the CECOFAD project." Collective Volume of Scientific Papers 72(2): 391-405.
Gaertner, D., S. Clermidy, et al. (2016). "Results achieved within the framework of the EU research project: Catch, Effort, and eCOsystem impacts of FAD-fishing (CECOFAD)." Acta Agriculturae Slovenica.
Hampton, I. (1996). "Acoustic and egg-production estimates of South African anchovy biomass over a decade: comparisons, accuracy, and utility." ICES Journal of Marine Science 53(2): 493-500.
ICCAT (2019). Report of the 2019 ICCAT yellowfin tuna stock assessment meeting., (Grand-Bassam, Cote d'Ivoire, 8-16 July 2019).
ICCAT (2021). Report of the 2021 ICCAT bigeye tuna stock assessment meeting., (Online, 19- 29 July 2021)
ICES (2015). Manual for International Pelagic Surveys (IPS). Series of ICES Survey Protocols. SISP 9 - IPS. 92 pp.
Katara, I., Gaertner, D., Marsac, F., Grande, M., Kaplan, D., Urtizberea, A., Abascal, F. (2018). Standardisation of yellowfin tuna CPUE for the EU purse seine fleet operating in the Indian Ocean. 20th session of the Working Party on Tropical Tuna.
Lo, N. C.-h., L. D. Jacobson, et al. (1992). "Indices of relative abundance from fish spotter data based on delta-lognornial models." Canadian journal of fisheries and aquatic sciences 49(12): 2515-2526.
Lopez, J., G. Moreno, et al. (2014). "Evolution and current state of the technology of echo-sounder buoys used by Spanish tropical tuna purse seiners in the Atlantic, Indian and Pacific Oceans." Fisheries Research 155: 127-137.
Masse, J., A. Uriarte, et al. (2018). "Pelagic survey series for sardine and anchovy in ICES subareas 8 and 9—Towards an ecosystem approach." ICES cooperative research report(332).
Maunder, M. N. and A. E. Punt (2004). "Standardizing catch and effort data: a review of recent approaches." Fisheries Research 70(2-3): 141-159.
Maunder, M. N., J. R. Sibert, et al. (2006). "Interpreting catch per unit effort data to assess the status of individual stocks and communities." ICES Journal of Marine Science 63(8): 1373-1385.
Moreno, G., L. Dagorn, et al. (2007). "Fish behaviour from fishers' knowledge: the case study of tropical tuna around drifting fish aggregating devices (DFADs)." Canadian journal of fisheries and aquatic sciences 64(11): 1517-1528.
Moreno, G., Dagorn, L., Capello, M., Lopez, J., Filmalter, J., Forget, F., Sancristobal, I., . and Holland, K. (2016). "Fish aggregating devices (FADs) as scientific platforms." Fisheries Research 178: 122- 129.
Orue, B., J. Lopez, et al. (2019). "From fisheries to scientific data: A protocol to process information from fishers' echo-sounder buoys." Fisheries Research 215: 38-43.
Orue, B., J. Lopez, et al. (2019). "Aggregation process of drifting fish aggregating devices (DFADs) in the Western Indian Ocean: Who arrives first, tuna or non-tuna species?" PloS one 14(1): e0210435.
Orúe Montaner, B. (2019). "Ecology and behavior of tuna and non-tuna species at drifting fish aggregating devices (DFADs) in the Indian Ocean using fishers' echo-sounder buoys."
Oshima, T. (2008). "Target strength of Bigeye, Yellowfin and Skipjack measured by split beam echo sounder in a cage." IOTC, WPTT-22 4.
Quinn, T. J. and R. B. Deriso (1999). Quantitative fish dynamics, oxford university Press.
Santiago, J., J. Uranga, et al. (2019). A Novel Index of Abundance of Juvenile Yellowfin Tuna in the Indian Ocean Derived from Echosounder Buoys, IOTC–2019–WPTT21–47.
Santiago, J., J. Uranga, et al. (2020a). A novel index of abundance of skipjack in the Indian ocean derived from echosounder buoys, IOTC-2020-WPTT22(DP)-14.

Santiago, J., J. Uranga, et al. (2020b). "A novel index of abundance of juvenile yellowfin tuna in the Atlantic Ocean derived from echosounder buoys." Collect. Vol. Sci. Pap. ICCAT 76(6): 321-343.

Santiago, J., J. Uranga, et al. (2021). " Index of abundance of juvenile bigeye tuna in the Atlantic Ocean derived from echosounder buoys (2010-2020)." Collect. Vol. Sci. Pap. ICCAT, 78(2): 231-252.

Scott, G. P., & Lopez, J. (2014). The use of FADs in Tuna Fisheries. European Parliament. Policy Department B: Structural and Cohesion Policies: Fisheries. IP/B/PECH/IC/2013.

Simmons, E. and D. MacLennan (2005). "Fisheries acoustics." Theory and Practice. Second edition published by Blackwell Science.

Team, R. C. (2013). R: A language and environment for statistical computing.

Torres-Irineo, E., D. Gaertner, et al. (2014). "Changes in fishing power and fishing strategies driven by new technologies: The case of tropical tuna purse seiners in the eastern Atlantic Ocean." Fisheries Research 155: 10-19.

Wain, G., Guéry, L., Kaplan, D. M., & Gaertner, D. (2021). "Quantifying the increase in fishing efficiency due to the use of drifting FADs equipped with echosounders in tropical tuna purse seine fisheries." ICES Journal of Marine Science 78(1), 235-245.

Wessel, P., and W. H. F. Smith (1996). " A global, self-consistent, hierarchical, high-resolution shoreline database." J. Geophys. Res 101(B4), 8741-8743.

TABLE 1. Technical specifications of different buoy models and observed values over analysis data.
TABLA 1. Especificaciones técnicas de diferentes modelos de boyas y valores observados sobre datos de análisis.

Model	Typical setup						Mean observed values over analysis data	
	Beam angle	Sounder frequency	Power	Frequency of acoustic sampling (ping rate)	Daily acoustic data recorded	Frequency of transmission	Number of buoys	Sampling frequency
DS+	32º	190.5 kHz	100 W	3	3	24h	1428	1.36
DSL+	32º	190.5 kHz	100 W	3	3	24h	12462	2.82
ISL+	32º	190.5 kHz	100 W	15 min	variable (reset at dusk)	24h	23	1.67
ISD+	32º	200/38 kHz (38 kHz not provided)	100 W	15 min	variable (reset at dusk)	24h	6214	1.21
SLX+	32º	200	100 W	5 min	variable (Sunrise or Alarms based)	24h	785	1.98

TABLE 2. Deviance table for the GLM lognormal model of the 2012-2023 period for SKJ.
TABLA 2. Tabla de desviación del modelo lognormal MLG del periodo 2012-2023 para SJK.

Variable	Df	Deviance	Resid..Df	Resid..Dev	F	Pr..F.	Variable	DevExp	Dev..Exp
NULL	NA	NA	6987	14555	NA	NA	NULL	NA	NA
yyqq	45	909	6942	13646	13	0.0000	yyqq	6	6.24 %
area	45	1038	6897	12608	15	0.0000	area	7	7.13 %
model	2	34	6895	12574	11	0.0000	model	0	0.23 %
den	1	25	6894	12549	16	0.0001	den	0	0.17 %
chl	1	10	6893	12539	7	0.0105	chl	0	0.07 %
chlfront	1	109	6892	12430	71	0.0000	chlfront	1	0.75 %
sst	1	5	6891	12425	3	0.0795	sst	0	0.03 %
sstfront	1	10	6890	12416	6	0.0115	sstfront	0	0.07 %
mld	1	0	6889	12416	0	0.9523	mld	0	0 %
yyqq:area	1311	3864	5578	8552	2	0.0000	yyqq:area	27	26.55 %

TABLE 3. Nominal and standardized Buoy-derived Abundance Index for the period 2012-2023, standard errors and coefficient of variations of the series.

TABLA 3. Índice de Abundancia Derivado de las Boyas nominal y estandarizado para el periodo 2012-2023, errores estándar y coeficiente de variaciones de la serie.

Buoy-derived Abundance Index for the period 2012-2023												
	SKJ				YFT				BET			
quarter	nominal	standarised	se	cv	nominal	standarised	se	cv	nominal	standarised	se	cv
12Q3	2.33	2.12	0.62	0.29	0.12	0.10	0.04	0.39	0.63	0.60	0.30	0.51
12Q4	1.54	1.41	0.41	0.29	0.15	0.21	0.08	0.39	0.45	0.34	0.17	0.51
13Q1	4.86	3.49	0.99	0.29	0.76	1.03	0.38	0.37	1.66	1.37	0.63	0.46
13Q2	3.23	1.92	0.46	0.24	0.65	0.37	0.12	0.33	1.73	0.88	0.39	0.44
13Q3	0.76	0.84	0.21	0.25	0.29	0.28	0.10	0.35	0.40	0.46	0.22	0.47
13Q4	1.00	0.69	0.18	0.26	0.28	0.26	0.09	0.36	0.54	0.29	0.14	0.47
14Q1	2.02	1.86	0.50	0.27	0.55	0.74	0.27	0.37	0.88	0.85	0.42	0.49
14Q2	1.46	1.54	0.39	0.25	0.59	0.60	0.22	0.36	0.80	0.65	0.32	0.50
14Q3	0.68	0.67	0.17	0.25	0.10	0.12	0.04	0.36	0.17	0.15	0.08	0.49
14Q4	1.12	1.07	0.28	0.26	0.18	0.24	0.09	0.36	0.25	0.35	0.17	0.49
15Q1	2.97	2.45	0.59	0.24	0.46	0.70	0.24	0.34	1.08	1.23	0.56	0.46
15Q2	1.84	1.60	0.37	0.23	0.49	0.64	0.20	0.32	0.71	0.61	0.26	0.42
15Q3	1.43	1.53	0.34	0.22	0.17	0.24	0.07	0.31	0.26	0.26	0.10	0.39
15Q4	0.99	1.19	0.27	0.22	0.16	0.21	0.06	0.31	0.26	0.42	0.17	0.40
16Q1	2.25	1.92	0.44	0.23	0.29	0.41	0.13	0.32	0.51	0.44	0.18	0.42
16Q2	1.07	1.08	0.26	0.24	0.13	0.14	0.05	0.34	0.32	0.28	0.13	0.45
16Q3	1.65	1.66	0.41	0.25	0.33	0.39	0.14	0.35	0.39	0.36	0.18	0.49
16Q4	2.35	2.05	0.51	0.25	0.33	0.45	0.16	0.36	0.55	0.34	0.17	0.50
17Q1	2.08	1.92	0.50	0.26	0.44	0.60	0.22	0.36	0.37	0.39	0.19	0.48
17Q2	1.40	1.40	0.33	0.24	0.40	0.52	0.17	0.33	0.46	0.35	0.15	0.43
17Q3	1.54	1.31	0.33	0.25	0.42	0.44	0.16	0.36	0.45	0.33	0.16	0.49
17Q4	1.87	1.56	0.42	0.27	0.47	0.61	0.22	0.37	0.27	0.34	0.17	0.50
18Q1	1.44	1.16	0.29	0.25	0.29	0.37	0.13	0.34	0.51	0.39	0.17	0.45
18Q2	1.25	1.06	0.26	0.24	0.35	0.45	0.15	0.33	0.38	0.28	0.12	0.43
18Q3	0.60	0.57	0.15	0.26	0.22	0.25	0.09	0.36	0.14	0.12	0.05	0.47
18Q4	2.06	1.52	0.37	0.24	0.31	0.42	0.14	0.34	0.50	0.36	0.16	0.45
19Q1	1.73	1.66	0.40	0.24	0.56	1.03	0.34	0.33	0.57	0.83	0.37	0.45
19Q2	1.90	1.68	0.41	0.24	0.42	0.44	0.15	0.34	0.69	0.63	0.28	0.45
19Q3	1.46	1.47	0.38	0.26	0.28	0.33	0.12	0.36	0.27	0.28	0.14	0.50
19Q4	2.23	2.29	0.57	0.25	0.62	0.64	0.22	0.35	0.37	0.48	0.23	0.47
20Q1	3.94	3.46	0.89	0.26	0.66	0.80	0.29	0.36	0.74	0.83	0.41	0.49
20Q2	2.91	2.65	0.65	0.24	0.55	0.58	0.20	0.35	0.88	0.60	0.28	0.47
20Q3	2.15	2.00	0.49	0.24	0.67	0.75	0.26	0.35	0.50	0.35	0.16	0.46
20Q4	2.39	2.20	0.53	0.24	0.54	0.68	0.23	0.34	0.25	0.22	0.10	0.47
21Q1	1.64	1.39	0.36	0.26	0.66	0.76	0.27	0.36	0.76	0.75	0.37	0.49
21Q2	1.28	0.85	0.21	0.25	0.15	0.15	0.05	0.34	0.47	0.28	0.13	0.46
21Q3	2.21	1.82	0.41	0.23	0.25	0.25	0.08	0.31	0.26	0.29	0.11	0.40
21Q4	1.19	1.19	0.31	0.26	0.28	0.37	0.13	0.35	0.09	0.23	0.10	0.44
22Q1	1.99	1.55	0.36	0.23	0.40	0.65	0.21	0.33	0.34	0.30	0.13	0.44
22Q2	1.27	1.37	0.33	0.24	0.79	0.71	0.24	0.34	0.37	0.40	0.18	0.44
22Q3	1.66	1.55	0.36	0.23	0.49	0.49	0.16	0.32	0.33	0.32	0.13	0.41
22Q4	1.43	1.47	0.33	0.23	0.54	0.57	0.17	0.30	0.24	0.26	0.10	0.37
23Q1	2.79	2.65	0.63	0.24	0.74	1.04	0.35	0.34	0.80	0.68	0.31	0.46
23Q2	3.90	3.23	0.78	0.24	0.88	1.30	0.45	0.34	0.81	0.73	0.34	0.46
23Q3	2.41	1.92	0.45	0.23	0.57	0.82	0.26	0.32	0.33	0.29	0.12	0.41
23Q4	2.29	2.28	0.56	0.24	0.60	0.67	0.23	0.35	0.20	0.28	0.13	0.47

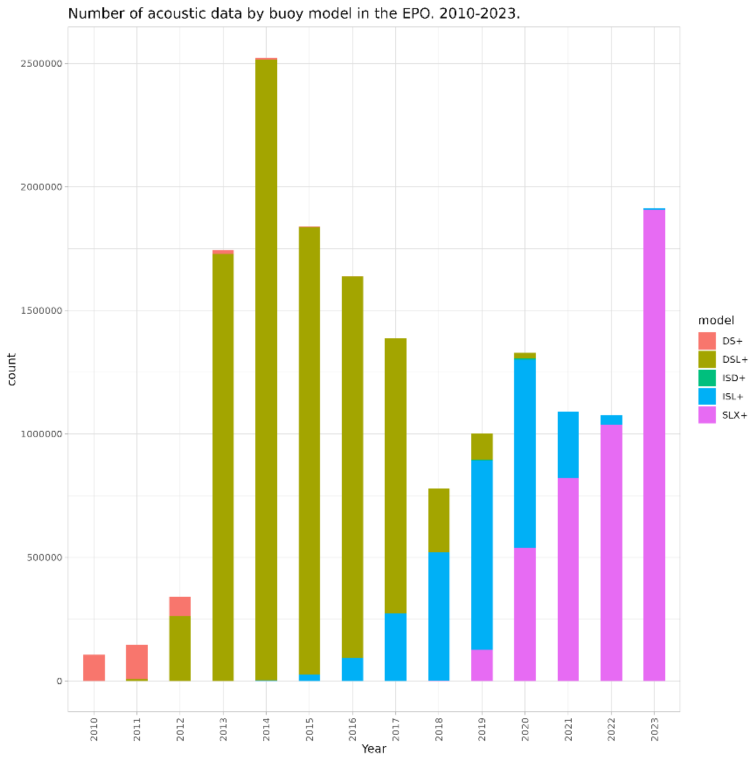

FIGURE 1. Buoy data distribution per model in the Pacific Ocean (2010-2023).
FIGURA 1. Distribución de datos de boyas por modelo en el Océano Pacífico (2010-2023).

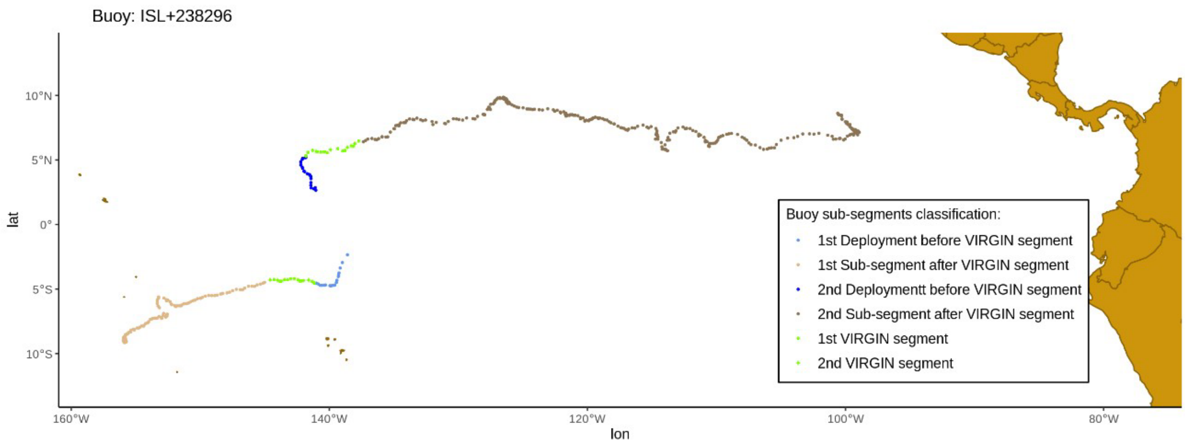

FIGURE 2. Example of "virgin" segments used for the calculation of the BAI index. Trajectories correspond to buoy ISL+284966 with two different paths representing drifts of different FADs. A virgin segment is defined as the segment of a buoy trajectory whose associated FAD likely represents a new deployment, which has been potentially colonized by tuna and not already fished. We consider as virgin segments (i.e. when tuna has aggregated to FAD) those segments of trajectories from 20-35 days at sea. "Virgin" segments are shown in green.

FIGURA 2. Ejemplo de segmentos "vírgenes" utilizados para el cálculo del índice IAB. Las trayectorias corresponden a la boya ISL+284966 con dos rutas distintas que representan derivas de diferentes plantados. Un segmento virgen se define como el segmento de la trayectoria de una boya cuyo plantado asociado probablemente representa una nueva siembra, que ha sido potencialmente colonizado por atunes y que aún no se ha pescado. Consideramos como segmentos vírgenes (es decir, cuando el atún se ha agregado a un plantado) aquellos segmentos de trayectorias de 20 a 35 días en el mar. Los segmentos "vírgenes" se muestran en verde.

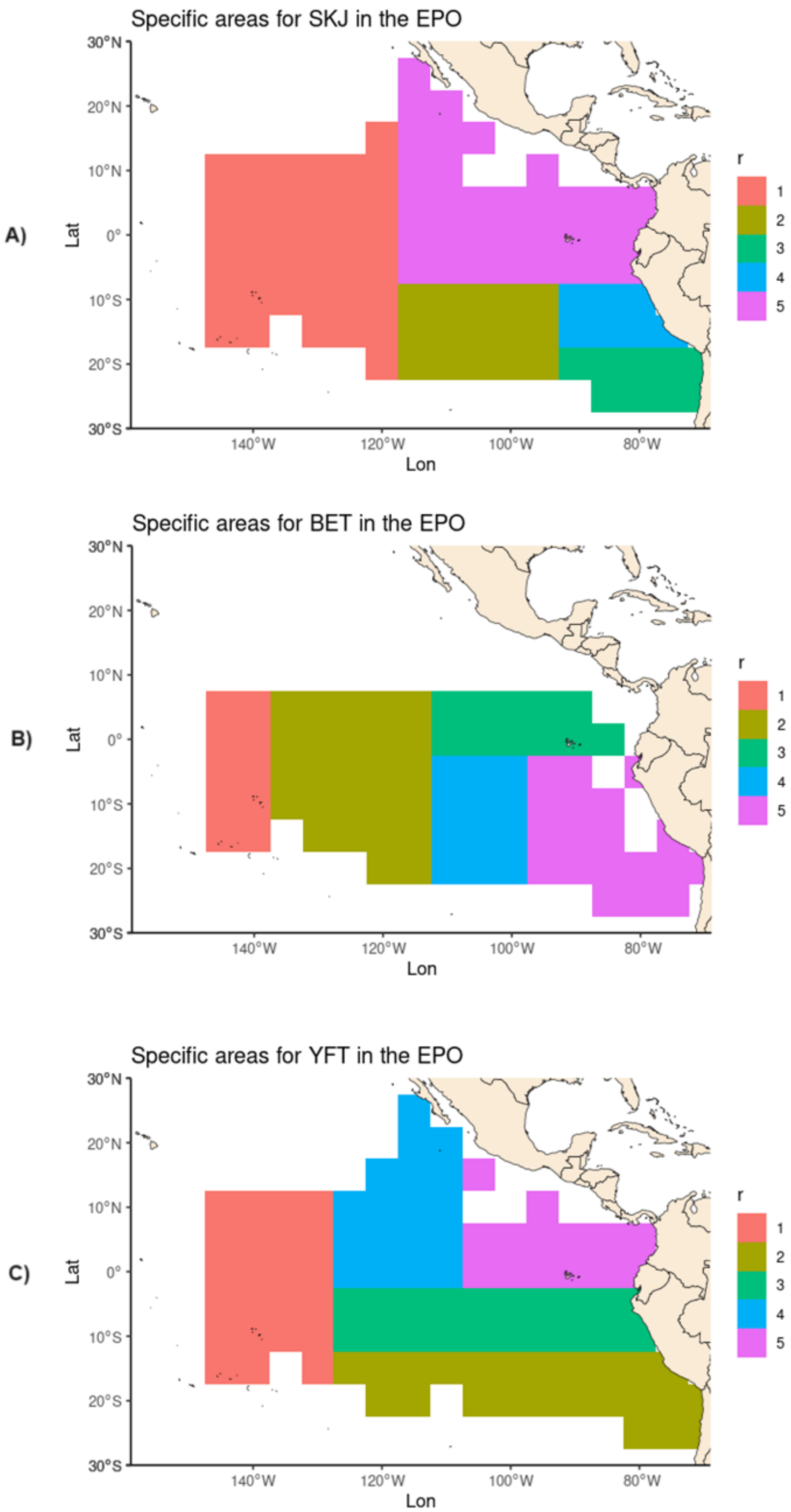

FIGURE 3. Length-frequency sampling areas defined by the IATTC staff for analyses of skipjack (A), bigeye (B) and yellowfin tuna (C) catches associated with floating objects.
FIGURA 3. Áreas de muestreo de frecuencia de tallas definidas por el personal de la CIAT para análisis de capturas de atunes barrilete (A), patudo (B) y aleta amarilla (C) asociadas con objetos flotantes.

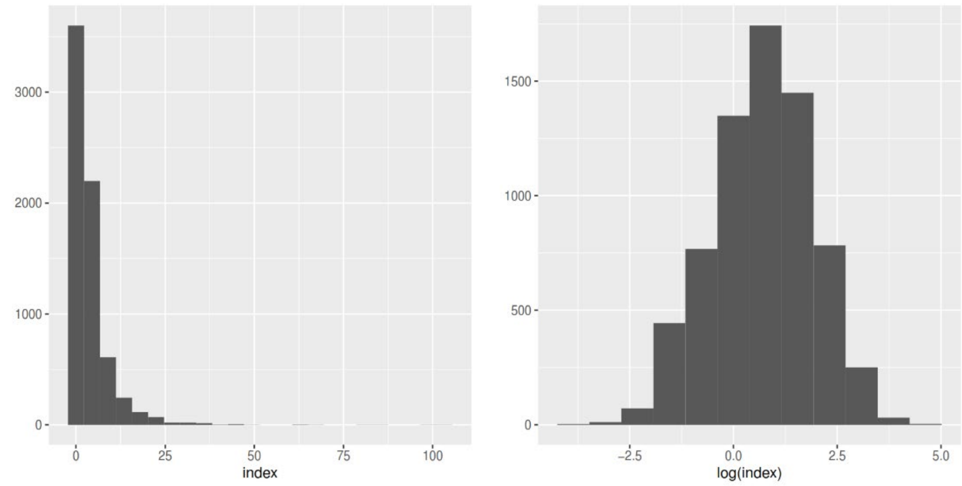

FIGURE 4. Histograms of the nominal values (left) and the log transformed nominal values (right) of the Buoy-derived Abundance Index for the SKJ (0.9 quantile of the integrated acoustic energy observations in "virgin" sequences).

FIGURA 4. Histogramas de los valores nominales (izquierda) y los valores nominales transformados logarítmicamente (derecha) del Índice de Abundancia Derivado de las Boyas para el SKJ (cuantil de 0.9 de las observaciones de energía acústica integrada en secuencias "vírgenes").

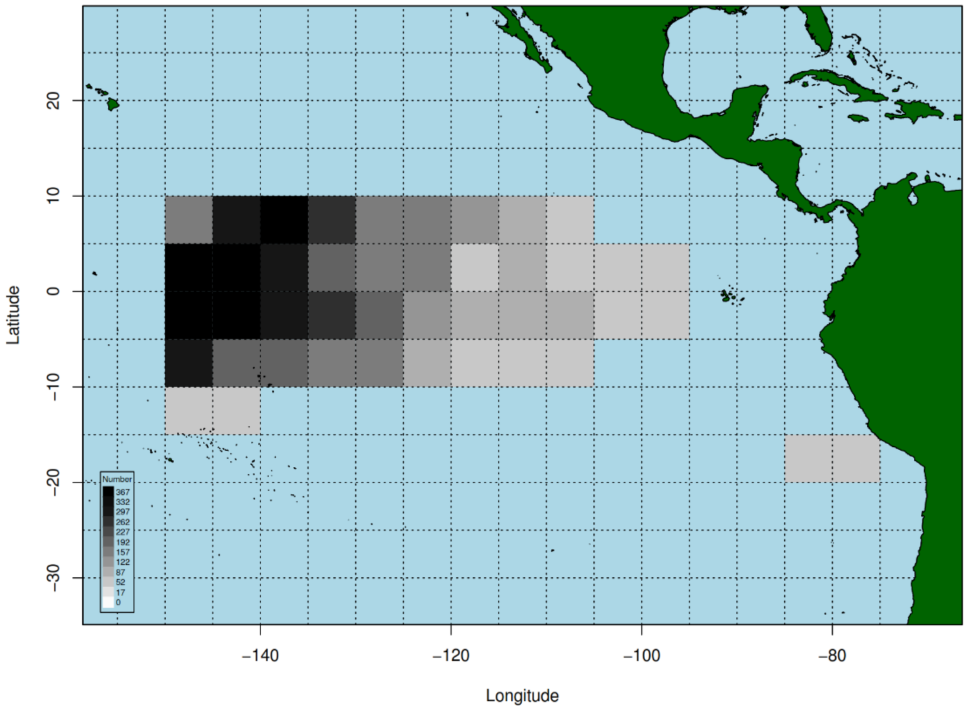

FIGURE 5. Spatial distribution [5ºx5º] of the "virgin" sequences of buoy trajectories that have been used in the GLM analysis for the SKJ.

FIGURA 5. Distribución espacial [5ºx5º] de las secuencias "vírgenes" de trayectorias de boyas que se han utilizado en el análisis MLG para el SKJ.

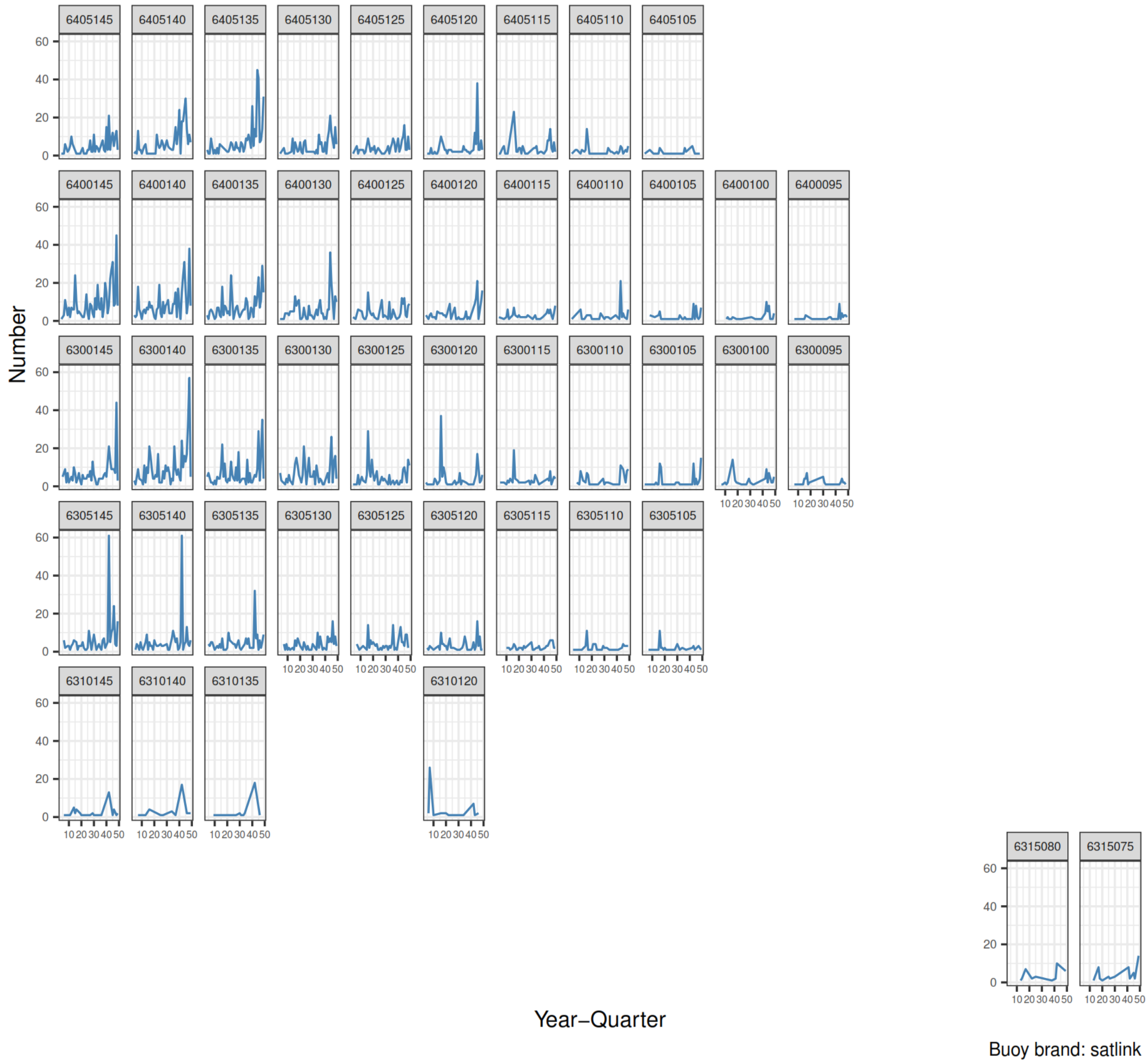

FIGURE 6. Quarterly evolution of the number of observations ("virgin" sequences of buoy trajectories) on a 5ºx5º grid from 2012 to 2023 for the SKJ.
FIGURA 6. Evolución trimestral del número de observaciones (secuencias "vírgenes" de trayectorias de boyas) en una cuadrícula de 5ºx5º de 2012 a 2023 para el SKJ.

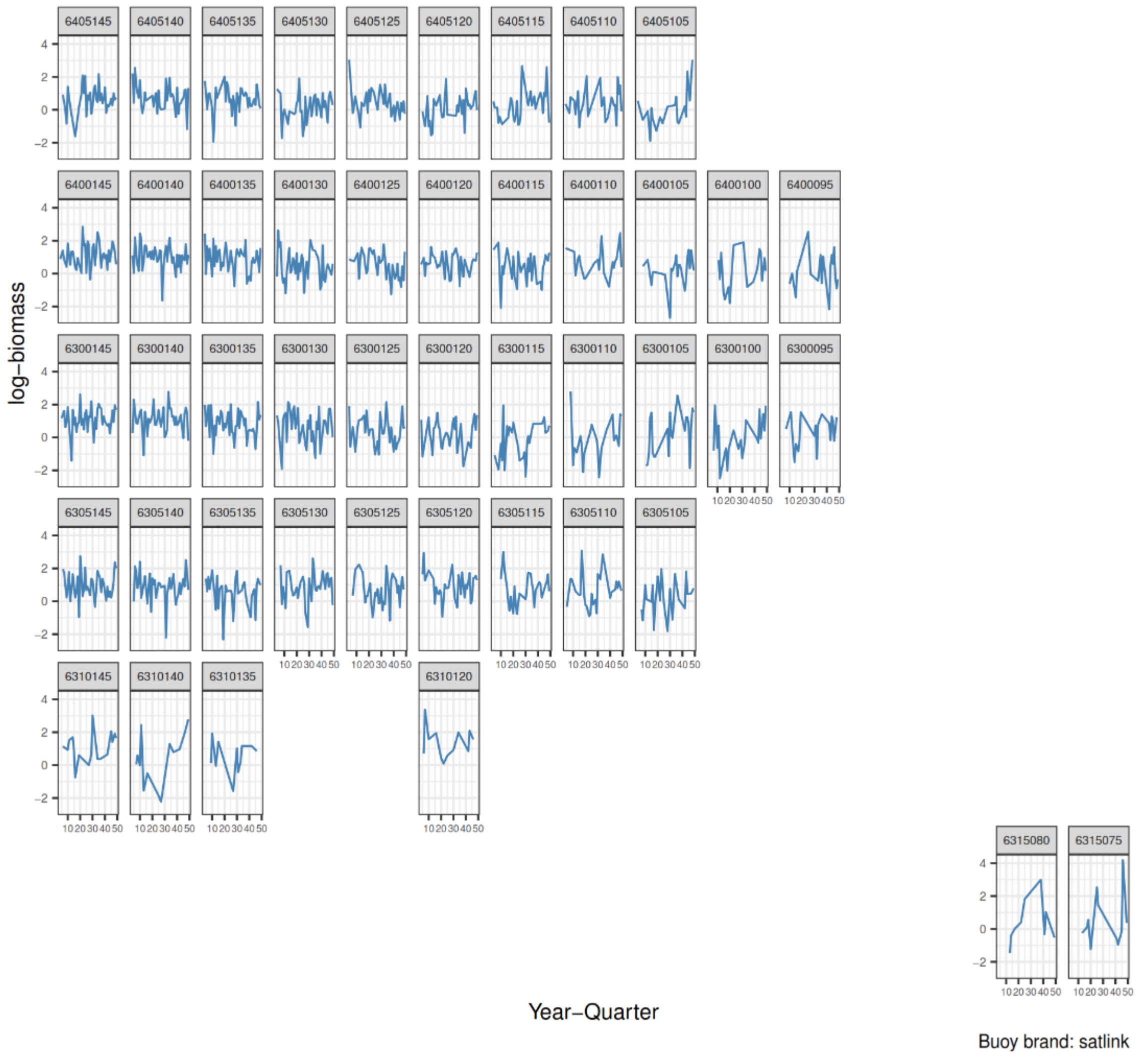

FIGURE 7. Quarterly evolution of the nominal log BAI index in the Atlantic Ocean by squares of 5x5 degrees from 2012 to 2023 for the SKJ.

FIGURA 7. Evolución trimestral del índice IAB logarítmico nominal en el Océano Atlántico por cuadrados de 5x5 grados de 2012 a 2023 para el SKJ.

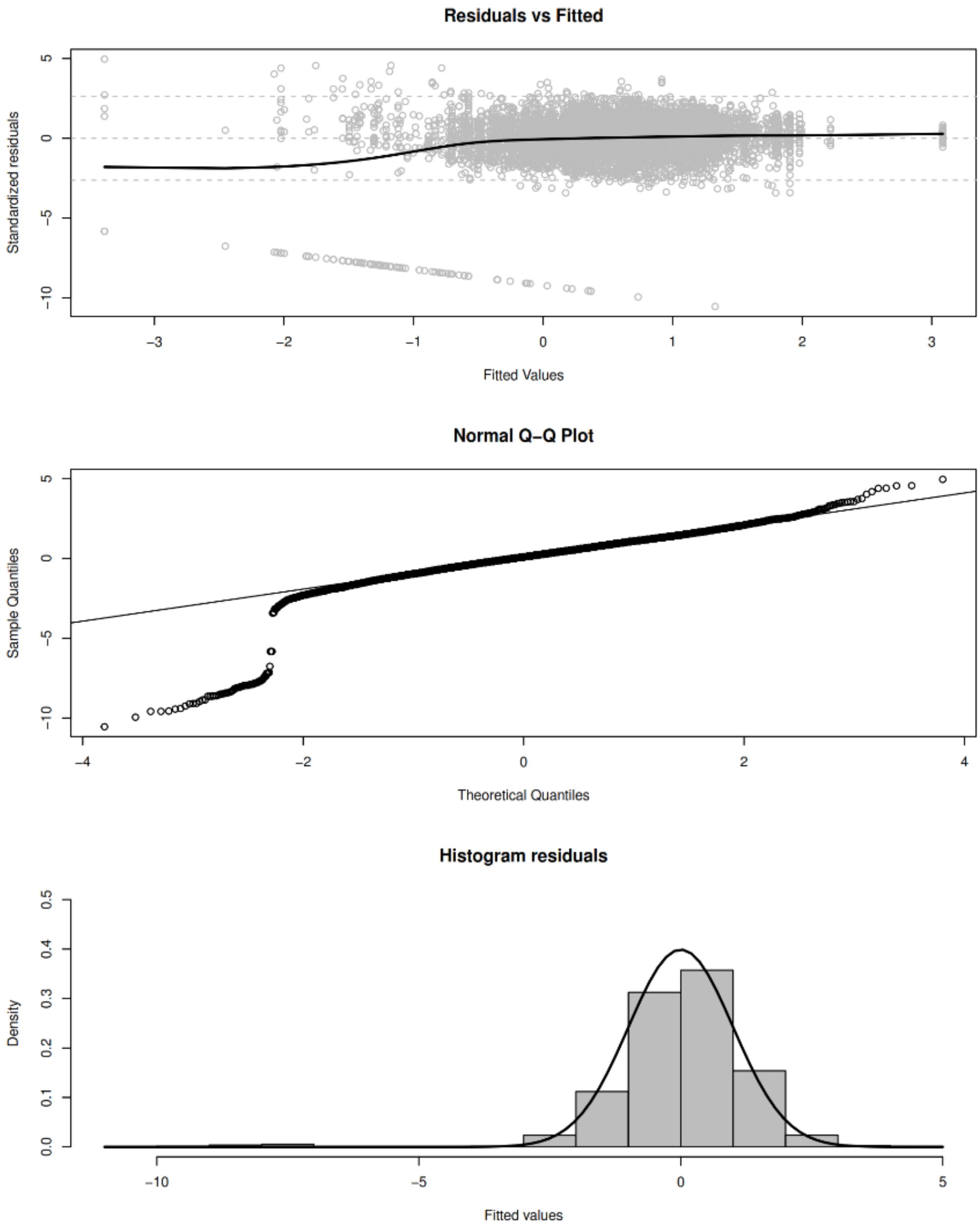

FIGURE 8. Diagnostics of the lognormal model selected for the period 2012-2023 for the SKJ: residuals vs fitted, Normal Q-Q plot and frequency distributions of the residuals.
FIGURA 8. Diagnóstico del modelo lognormal seleccionado para el periodo 2012-2023 para el SKJ: residuales vs. ajustados, gráfico Q-Q normal y distribuciones de frecuencia de los residuales.

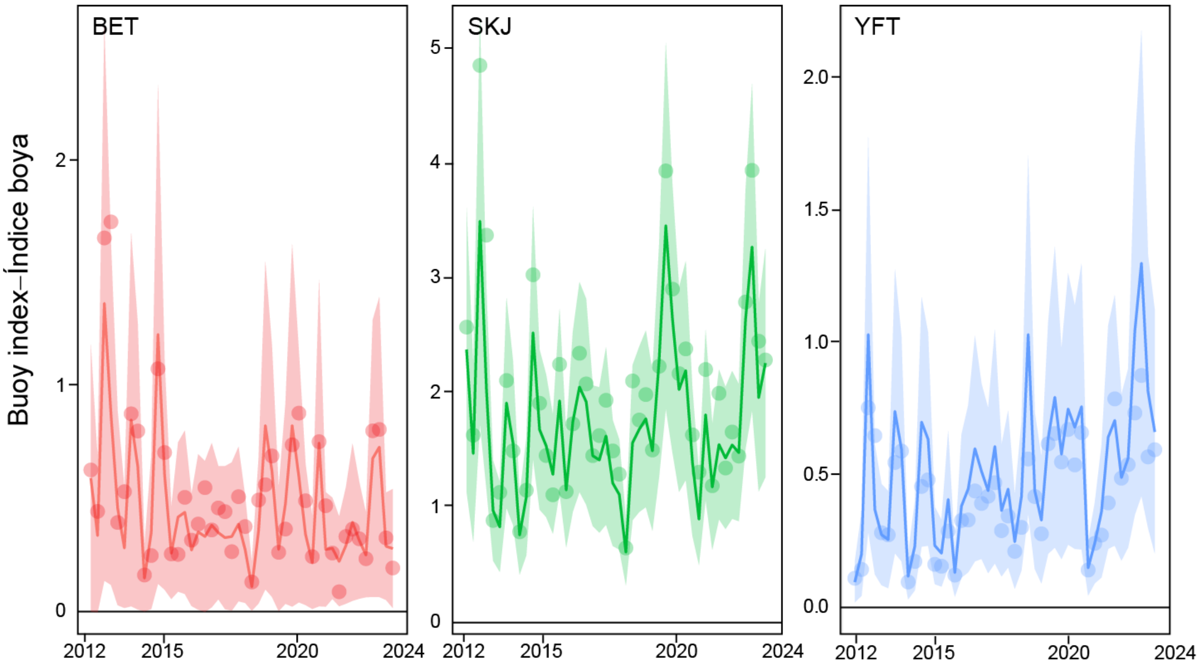

FIGURE 9. Time series of nominal (circles) and standardized (continuous line) Buoy-derived Abundance Index for the period 2012-2023 for all three tropical tuna species. The 95% upper and lower confidence intervals of the standardized BAI index are shown by the grey shaded area.

FIGURA 9. Serie de tiempo del Índice de Abundancia Derivado de Boyas nominal (círculos) y estandarizado (línea continua) para el periodo 2012-2023 para las tres especies de atunes tropicales. Los intervalos de confianza superior e inferior del 95% del índice IAB estandarizado se muestran en el área sombreada en gris.